STUDY OF CRYSTALLINE-PHASE FORMATION IN WHITE ZIRCONIUM GLAZES

(*)Escardino, A.; (*)Moreno, A.; (*)Amorós, J.L.; (*)Gozalbo, A.
(**)Aparici, J.; (**)Sánchez, L.F.

(*) Instituto de Tecnología Cerámica.
Asociación de Investigación de las Industrias Cerámicas.
Universitat Jaume I. Castellón. Spain.
(**) ESMALGLASS S.A

ABSTRACT

The nature of the crystalline phases that devitrify on heat treating test specimens formed from an industrial zirconium frit, has been determined. Zircon was shown to be the crystalline phase that produces the whiteness of the glaze coatings obtained on firing this frit.

Several series of experiments were carried out with a view to studying the devitrification kinetics of zircon crystals, under nonisothermal conditions (at a constant rate of heating), using test specimens formed by casting from a frit particle-size fraction similar to the one that is usually applied (by the wet method) to the ceramic body, in glazed ceramic tile manufacture.

In this study, on using a kinetic model derived from isothermal crystallization experiments, set out elsewhere, which were performed with the same frit and particle-size fraction, it has been possible to reproduce the experimental results obtained.

1. INTRODUCTION

The frits that give rise to opaque glazes are used in the ceramic floor and wall tile industry to produce glossy or matt white glaze coatings. They can also be used as constituents for the engobe that is usually applied between the glaze and the body for different purposes.

The phenomenon of opacification in glazed ceramic tile, arises as a result of the scatter of incident light rays on hitting micro-heterogeneities throughout the glassy phase. These heterogeneities are usually crystalline phases or immiscible liquid phases.

Most white ceramic glazes are obtained from zirconium frits. In these frits, opacity arises as a result of the devitrification of several crystalline phases during the firing cycle to which the ceramic tile is subjected [1]. The major crystalline phase that forms is zirconium silicate or zircon. Variable quantities may also be encountered of diopside, wollastonite, etc., depending upon the chemical composition of the starting frit composition.

The use of zirconium glazes for ceramic floor and wall tile coatings, is not only due to their high whiteness index, but also to their excellent mechanical and chemical properties, as well as their adaptability to the firing cycles that are usually employed in industry. In these glazes, a proportionality has been found to exist between the whiteness index (linked to opacity), and the nature, proportion and mean size of the crystals that the glazes contain [2].

As a result of the fact that glazed tiles undergo nonisothermal industrial firing cycles, and that the devitrification of crystalline phases in the glaze layer arises during the heating step and perhaps during the firing cycle peak temperature step [2], it was felt of interest to study the kinetics of zircon crystal formation under nonisothermal conditions, at a constant rate of heating.

A study was therefore undertaken, with a view to determining:

a) The nature of the crystalline phases that devitrify during heat treatment of a zirconium frit;

b) The crystalline phases that yield the whiteness of the glaze coating obtained on firing a tile that has been glazed using the above frit, by means of the same method that is employed in glazed ceramic tile manufacture;

c) The kinetics of the devitrification process when this takes place under nonisothermal conditions, while keeping a constant rate of heating, in order to make the experimental operating conditions approach actual industrial kiln operating conditions, during the heating step of the firing cycle for ceramic tile manufacture.

2. EXPERIMENTAL PROCEDURE

The study was carried out by using a zirconium frit fabricated by ESMALGLASS, S.A., which contained the following constituents (expressed as oxides): ZrO_2 (round 9% by weight); CaO, MgO, Al_2O_3, SiO_2, ZnO and B_2O_3.

X-ray diffraction (XRD) was used to determine the crystalline-phase content of the resulting glaze coatings, while using scanning electron microscopy (SEM) and EDX analysis to determine their microstructure and the nature of the crystalline phases that they contained. In the starting frit, small quantities of zircon crystals and monoclinic ZrO_2 were detected by XRD.

The industrial frit was wet milled in a laboratory ball mill, until a suspension with the targeted particle-size distribution was obtained.

In order to determine the temperature interval at which devitrification occurred on heating the frit, DTA tests were run at different heating rates: 2, 5, 10 and 50°C/min., using samples with varying mean particle sizes.

In the experiments carried out to identify the crystalline phases present after firing and to study devitrification kinetics, cylindrical test specimens were used, which were 11 μm thick with a diameter of 11 μm (when unfired), formed by casting from a suspension of frit particles sized below 40 μm, whose particle-size distribution is reported in Fig. 1. After drying, the test specimens were fired in an electric laboratory kiln (CARBOLITE RHF 1400), using variable temperature cycles, at heating rates of 2.5, 5, 10 and 50°C/min respectively.

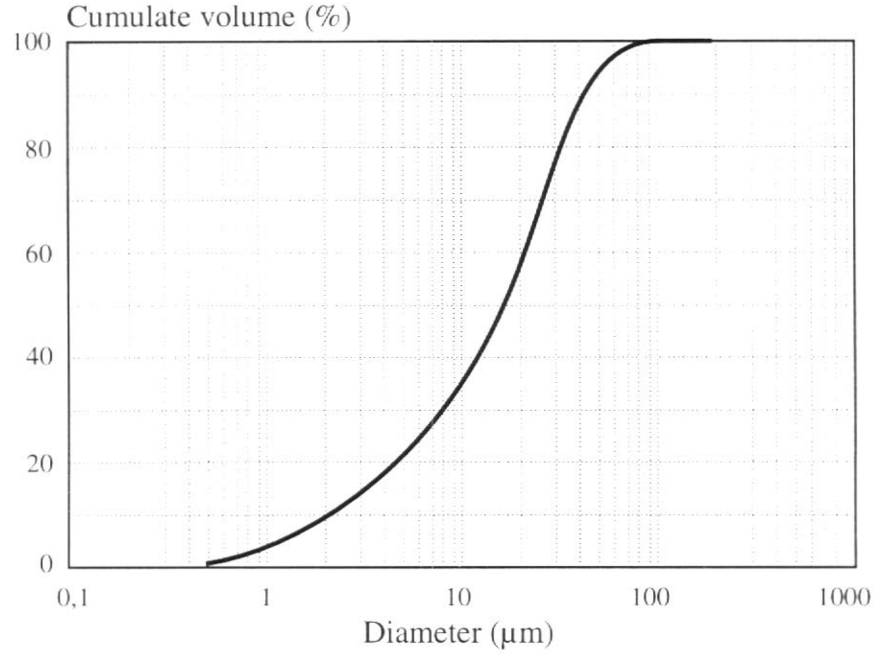

Figure 1. *Particle-size distribution of the frit used for preparing the test specimens.*

In each experiment, the test specimen was placed in the kiln at room temperature. Heating then followed at a rate of 50°C/min up to 160°C. This temperature was held for 1.5 min, followed by renewed heating at a rate of 50°C/min up to 300°C. From this point on, kiln temperature was raised at the set constant rate of heating: 2.5, 5, 10 or 50°C/min. The test specimens were withdrawn from the kiln when the kiln reached different peak temperatures, which ranged from 850 to 1250°C, subsequently cooling the specimens in air. It had been substantiated by testing beforehand, that rapid cooling of the test specimens by water quenching yielded the same results as when they were air cooled.

To determine temperature at the surface (T_s) and within the cylindrical test specimens (T_i), during the firing cycle, the setup depicted in Fig. 2 was used, in which thermocouples were employed, fitted with compensating extension wires that reached up to the measuring device, which was located sufficiently far away from the kiln to assure that the cold junction would remain at room temperature.

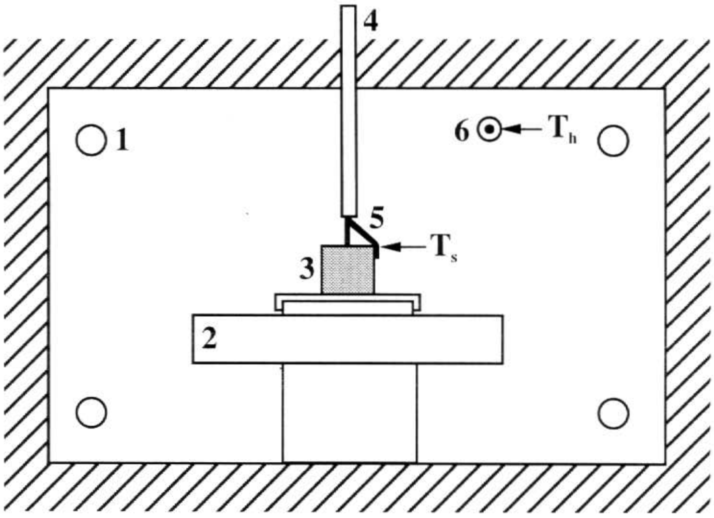

1. Resistances
2. Refractory base
3. Frit button
4. Alumina tube
5. Thermocouples
6. Kiln thermocouples

Figure 2. *Setup used for determining the variation of* T_h, T_s *and* T_i.

As the test specimens formed from the selected frit partially fused at round 850°C, the following was done in order to prevent any deterioration from arising of the thermocouples used in the experiments aimed at comparing the evolution of T_s and T_i, with the temperature indicated by the thermocouple located inside the kiln (T_h), at temperatures ranging from 850 to 1200°C:

a) A series of experiments was conducted at each of the four selected heating rates, using test specimens made from the zirconium frit. In each series, the experiments were stopped when kiln temperature reached 850°C.

b) Another series of four experiments was run under analogous operating conditions to the former, using cylindrical test specimens of the same size, formed from a refractory material, which withstood temperature better, with a similar density and surface quality to those of the test specimens formed from frit particles. These experiments were run up to 1200°C. The values of T_i obtained in this second series were much less representative than those of the foregoing series, because the thermal conductivities of the specimens made from the frit and the refractory material were different.

The nature and proportion of the crystalline phases present in the fired frit test specimens were determined by XRD. The zircon crystal content of these test specimens was assessed from the number of counts at the 3.30 Å peak corresponding to this phase, using a calibrating straight line. The monoclinic zirconium oxide content of the starting frit was similarly determined, by using its maximum intensity peak, located at 3.16 Å.

3. RESULTS AND DISCUSSION

3.1. NATURE OF THE DEVITRIFYING PHASES

3.1.1. DTA testing

i) Influence of mean particle size

Fig. 3 depicts the thermograms obtained from different particle-size fractions of the selected frit, corresponding to size intervals: Dp<40μm; 40<Dp<60μm and 125<Dp<200μm, using a heating rate of 10°C/min. In the three cases, a wide exothermic band forms, in which several peaks appear at different temperatures, which may represent the devitrification of as many crystalline phases. As mean particle size rises, this band is shifted towards the highest temperature region, and becomes flatter.

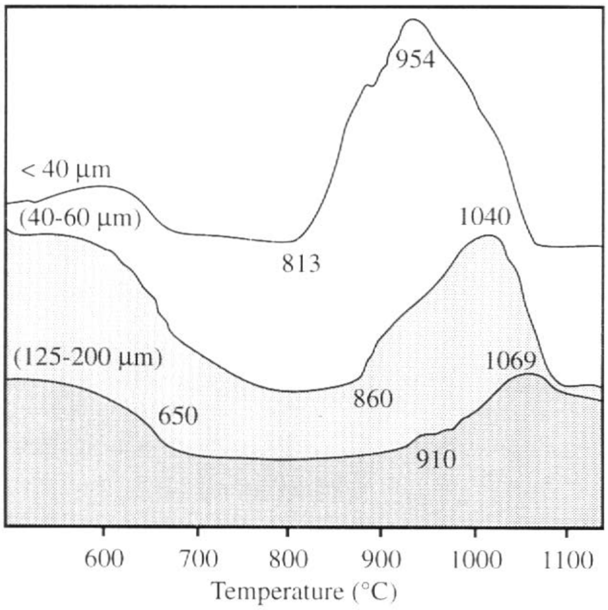

Figure 3. *DTA curves corresponding to fractions Dp<40μm, 40<Dp<60μm and 125<Dp<200μm of the frit. Heating rate 10°C/min.*

As frit mean particle size appears to influence the crystallization process, the remaining study was carried out using a particle-size fraction of <40μm, which corresponds to the particle-size distribution that is usually employed industrially when such a frit is applied as an aqueous suspension to the ceramic body, in glazed tile manufacture.

ii) DTA determination of the temperature interval at which crystalline phases form.

Fig. 4 reports the thermograms obtained on using heating rates of 2.5, 5, 10 and 50 °C/min, with a frit particle-size fraction sized below 40μm. It can be observed that the temperature interval at which crystalline phases devitrify, obtained from the width of the previously mentioned exothermic band, lies in the 800-1150°C range, at the four tested heating rates. The highest peak in the band, corresponding to peak crystallization rate, shifts slightly towards the higher temperature region, as the heating rate increases.

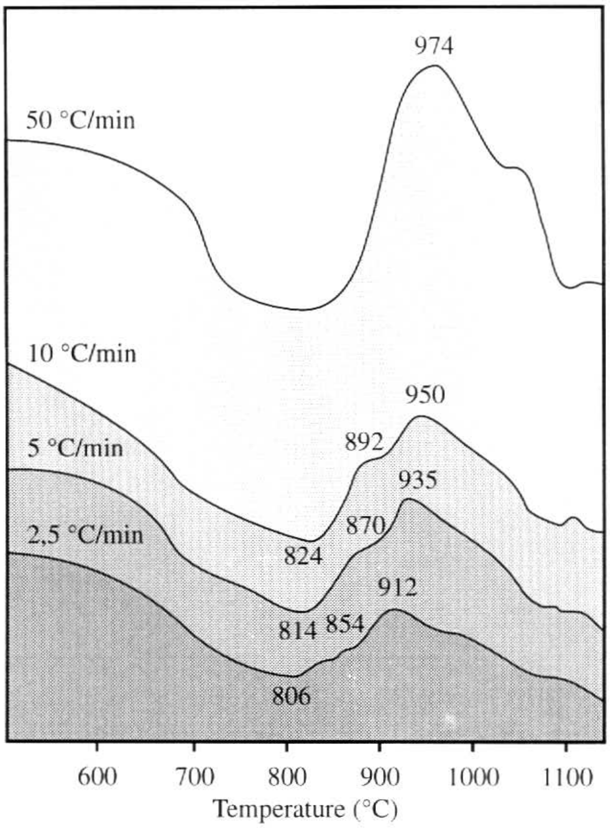

***Figure 4**. DTA thermograms obtained, corresponding to different heating rates*

3.1.2. SEM examination of glaze microstructure

Fig. 5 shows the photograph of a test specimen that has been isothermally treated at 900°C for 320 min, in which some domains have been highlighted, identifying the observed crystalline phases. The existence can be observed of crystals of differing appearance within the glassy phase; the nature of these crystals was determined by EDX analysis.

Monoclinic zirconium oxide crystals are visible in the centre of the photograph, which are almost white, with rounded edges, sized between 3 and 5μm. The dark grey regions correspond to crystals with a diopside structure (calcium and magnesium silicate), which might contain petedunite (zinc and calcium silicate). The light grey areas correspond to the zircon structure (zirconium silicate). The striped areas represent the glassy phase.

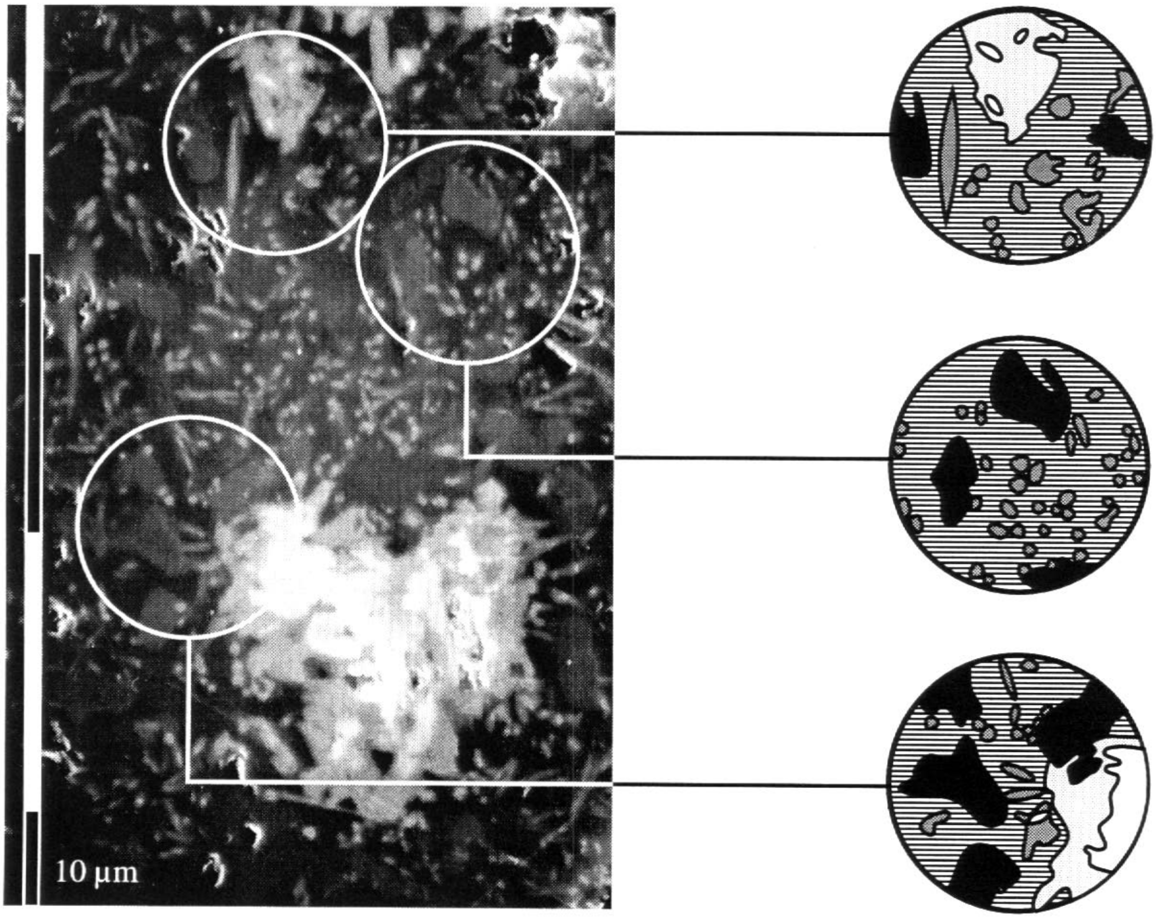

○ ZrO_2 ○ $ZrSiO_4$ ◉ Cristalline phases made up of ZrO_2 and/or $ZrSiO_4$ ● Diopside ⊜ Glassy phase

Figure 5. *Nature of the devitrifying crystalline phases*

3.1.3. Identification by XRD of the arising crystalline phases

Fig. 6 depicts the XRD diffractograms corresponding to the different heat-treated test specimens, at a heating rate of 5°C/min, up to various peak temperatures.

In the diffractogram corresponding to the test specimen heated up to 800°C, the presence of zircon and monoclinic ZrO_2 can be observed in proportions that practically coincide with those detected in the starting frit, which suggests that the devitrification process has not as yet commenced at this temperature.

In the diffractogram of the test specimen heated up to 850°C, diopside and tetragonal ZrO_2 are observed to have started crystallizing. while the previously observed zircon and monoclinic zirconia peaks appear to have undergone no change in respect of the former peaks.

The proportions of monoclinic and tetragonal ZrO_2, and diopside progressively increase as cycle end temperature is raised, peaking at round 1000°C. At this temperature, the presence of zircon starts becoming noticeable.

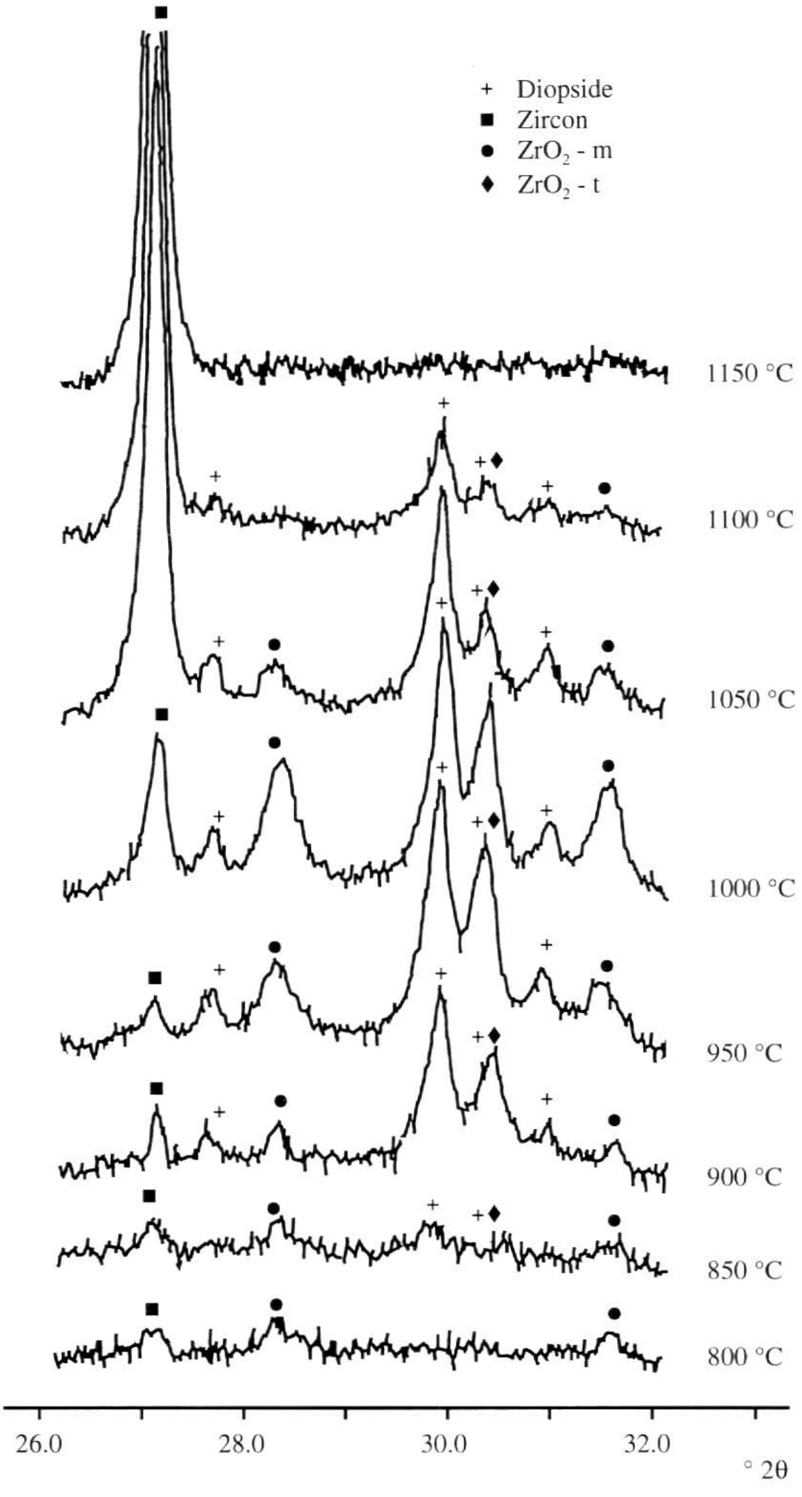

***Figure 6**. Crystalline phases identified at different peak temperatures. Heating rate 5 °C/min.*

On continuing to raise temperature above 1000°C, monoclinic and tetragonal zirconium oxides disappear, forming zirconium silicate. Diopside also disappears, so that the only phase found in considerable proportions at 1150°C is zirconium silicate. The crystalline phases that were identified by XRD coincided with the ones detected by EDX analysis, discussed in the foregoing section.

3.2. CRYSTALLINE PHASES YIELDING WHITENESS IN THE STUDIED ZIRCONIUM GLAZE

The data set out above allow inferring that when the studied frit is used for obtaining white glaze coatings for ceramic tile, operating under the usual firing conditions in ceramic floor and wall tile manufacture ($1110°C < T_{max} < 1140°C$ with particles sized below 40µm), the only crystalline phase that can be present in such glazes is zircon, possibly accompanied by a small amount of diopside. Therefore, opacity and consequently the whiteness index of the glaze must depend largely on its zircon crystal content.

This outcome is consistent with what had previously been observed for this kind of glaze, as it had been shown that its whiteness index rose with the zircon content, tending asymptotically to a peak value that is usually found when the zircon mass fraction in the glaze is 0.16 [2].

3.3. KINETIC STUDY

3.3.1 Experimental results

Tables I to IV show the results obtained. The amount of crystallized zircon, in each case, has been assessed as the zirconium fraction contained in the starting frit, which became zirconium silicate, expressed in molar units:

$$n_{sz} = \frac{\textbf{moles of crystallized zirconium silicate}}{\textbf{at - g of zirconium initially present in the test specimen}} =$$

$$= \frac{\textbf{at - g of zirconium contained in the crystalline phase (zircon)}}{\textbf{at - g of zirconium initially present in the test specimen}}$$

as each mole of crystallized zirconium silicate contains one at-g of zirconium.

These tables detail the values of n_{sz} together with those corresponding to the test specimen kiln dwell time (t), and the temperature value measured by the thermocouple located within the kiln (T_h). Dwell time was measured starting from the moment at which kiln temperature reached 300°C (T_0) and the constant-rate-of-heating period started.

Table I. *Heat-treatment cycle no. 1 (a=2.5°C/min) Variation of n_{sz} with t and T_h*

t (min)	T_h (°C)	n_{sz}
0	300	0,02
220	850	0,02
240	900	0,03
260	950	0,04
270	975	0,09
280	1000	0,16
290	1025	0,39
300	1050	0,75
312	1080	0,97
320	1100	0,99

Table II. *Heat-treatment cycle no. 2 (a=5°C/min) Variation of n_{sz} with t and T_h*

t (min)	T_h (°C)	n_{sz}
0	300	0,02
110	850	0,02
120	900	0,02
130	950	0,03
140	1000	0,05
145	1025	0,14
150	1050	0,36
155	1075	0,70
160	1100	0,85
165	1125	0,96
170	1150	0,96

Table III. *Heat-treatment no. 3 (a=10°C/min) Variation of n_{sz} with t and T_h*

t (min)	T_h (°C)	n_{sz}
0	300	0,02
55	850	0,02
60	900	0,08
65	950	0,05
67,5	975	0,04
70	1000	0,05
72,5	1025	0,07
75	1050	0,21
75,5	1075	0,51
80	1100	0,85
85	1150	0,96
90	1200	0,94

Table IV. *Heat-treatment cycle no. 4 (a=50°C/min) Variation of n_{sz} with t and T_h*

t (min)	T_h (°C)	n_{sz}
0	300	0,02
11	850	0,02
12	900	0,04
13	950	0,03
14	1000	0,02
14,5	1025	0,03
15	1050	0,02
15,5	1075	0,05
16	1100	0,13
16,5	1125	0,38
17	1150	0,60
18	1200	0,85

3.3.2 Proposed model

Assuming that zircon crystallization takes place in three consecutive steps [3]:

$$\mathbf{Zr(v)} \xrightarrow[\mathbf{(I)}]{\mathbf{+O_2}} \mathbf{ZrO_2(v)} \xrightarrow[\mathbf{(II)}]{} \mathbf{ZrO_2(c)} \xrightarrow[\mathbf{(III)}]{\mathbf{+SiO_2}} \mathbf{SiO_4Zr(c)}$$

and making the assumption that step (I), in which the ZrO_2 (v) structural units are formed in the glassy phase from the Zr it contains, develops almost instantaneously, that step (II), involving ZrO_2 crystal formation, is controlled by the diffusion of ZrO_2 structural units (through the glassy phase) to the crystal-glass interface, and that step (III) takes place as though it were a quasi first order irreversible reaction in respect of the crystallized zirconium oxide that is present, a kinetic model has been proposed [3], which yields two differential equations of the form:

$$\frac{dn_z}{dt} = -D(n_z - n_z^e) \tag{1}$$

$$\frac{dn_{sz}}{dt} = k \cdot n_{oz} = k(1 - n_z - n_{sz}) \tag{2}$$

where:

n_z = mean fraction of the starting zirconium content that remains in the glassy phase (at.g of Zr in the glassy phase/at-g of Zr initially present in the system).

n^e_z = fraction of the starting zirconium content which is in equilibrium in the glass-crystal interface with the crystal (at.g of Zr in the glassy phase/at-g of Zr initially present in the system).

n_{oz} = fraction of the starting zirconium content that is present in the form of monoclinic or tetragonal zirconia crystals (mole of crystallized ZrO_2/at-g of Zr initially present in the system).

n_{sz} = fraction of the starting zirconium content that is present in the form of zirconium silicate crystals (mole of crystallized $ZrSiO_4$/at-g of Zr initially present in the system).

D = rate constant that includes the effective diffusivity of zirconium through the glassy phase, thickness of the boundary layer, test specimen volume, and n° of at-g of zirconium initially present in the test specimen (min^{-1}).

k = rate constant of the third step (min^{-1}).

t = kiln dwell time (min).

On simultaneously integrating these two differential equations, by the Runge-Kutta method of order 4, having established the values of D and k, the value of n^e_z and boundary conditions (values of n^0_z and n^0_{sz} for t=0), it is possible to calculate the variation of n_z and n_{sz} with kiln dwell time, at a given test specimen temperature.

The effectiveness of this kinetic model was substantiated elsewhere [3] using data from several series of isothermal experiments run at different temperatures (ranging from 850 to 1000°C), modifying, in each experiment, the dwell time of the test specimens, that were formed from particles of the same frit, which had an identical particle-size distribution to the ones used in the experiments that have been carried out in this study.

On using differential Equations (1) and (2) to fit the experimental data obtained at various temperatures, in the study indicated [3], yielded a series of values for constants D and k, that satisfactorily fitted equations of the form:

$$D = A_1 \cdot \exp\left[-\frac{E_1}{RT}\right] \text{ y } k = A_2 \cdot \exp\left[-\frac{E_2}{RT}\right] \tag{3}$$

where T is test specimen temperature expressed in K. For parameters A_i and E_i (i=1, 2) the following values were obtained:

$A_1 = 9.00 \times 10^9\ min^{-1}$; $E_1/R = 33{,}500$ K
$A_2 = 6.72 \times 10^{12}\ min^{-1}$; $E_2/R = 40{,}700$ K

For the variable n^e_z, the mean value 0.02 was derived.

3.3.3 Fit of the proposed model to the experimental results obtained in this study

Using Equations (1), (2) and (3), it was attempted to reproduce the experimental data found under nonisothermal conditions, at the four tested heating rates. This was done by rewriting them in the form:

$$\frac{dn_z}{dt} = -A_1 \cdot \exp\left[-\frac{E_1}{R}\left(\frac{1}{273+T}\right)\right](n_z - n^e_z) \tag{4}$$

$$\frac{dn_{sz}}{dt} = A_2 \cdot \exp\left[-\frac{E_2}{R}\left(\frac{1}{273+T}\right)\right](1 - n_z - n_{sz}) \tag{5}$$

In order to integrate these equations, the assumption was made, firstly, that test specimen temperature (T), for each kiln dwell time value (t), practically coincided with the temperature that was measured in the kiln (T_h) expressed in °C, corresponding to that time t.

Thus, temperature (T), which appears in these equations, was substituted by:

$$\mathbf{T = T_h = 300 + a \cdot t \qquad (°C)}$$

where $T_0=300$ represents the value of T_h for $t=0$, since measurement of this last variable started in every experiment at $T=300°C$, as indicated above. The symbol ***a*** represents the constant rate of heating used in each series of conducted experiments.

Thus, in accordance with the foregoing, differential Equations (4) and (5) became:

$$\frac{dn_z}{dt} = -A_1 \exp\left[-\frac{E_1}{R}\left(\frac{1}{573 + a\_t}\right)\right](n_z - n_z^e) \tag{6}$$

$$\frac{dn_{sz}}{dt} = -A_2 \exp\left[-\frac{E_2}{R}\left(\frac{1}{573 + a \cdot t}\right)\right](1 - n_z - n_{sz}) \tag{7}$$

On substituting the values of A_1, A_2, E_1/R and E_2/R proposed above into these equations, and operating $n^e_z=0.02$, the equations were then integrated, after assigning to variable ***a*** (heating rate) the value corresponding to the series of experiments whose results it was intended to try and reproduce.

The boundary conditions used were $t=0$; $n^0_z=0.89$ and $n^0_{sz}=0.02$. These last two values were computed from the XRD analysis results of the starting frit, that contained small amounts of ZrO_2 ($n^0_{oz}=0.09$) and zircon crystals ($n^0_{sz}=0.02$). The value of n^0_z was derived by mass balance from n^0_{oz} and n^0_{sz}:

$$n^0_z = 1 - n^0_{oz} - n^0_{sz}$$

Operating in this way, the values of n^0_{sz} were obtained, which have been plotted versus kiln dwell time in Fig. 7, using solid lines, together with the experimental outcomes (Tables I to IV), for the four tested heating rates.

It can be observed that the values of n_{sz}, calculated in this fashion, by integrating Equations (6) and (7), match the experimental data quite well.

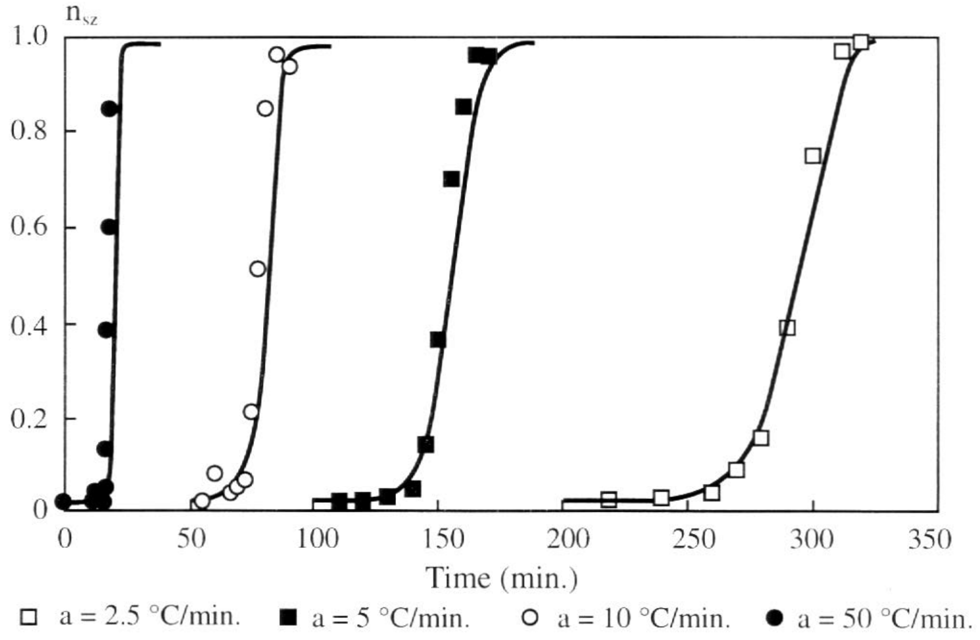

Figure 7. *Plot of the experimental data (points) and values calculated from Eqs. (6) and (7) (solid lines), for each studied heating rate.*

3.3.4 Temperature correction

In a foregoing article [4], it was shown that the temperature measured by the kiln thermocouple (T_h) was slightly lower than the temperature at the test specimen surface (T_s), and that the difference between both temperatures depended on the heating rate employed. It was also shown that the devitrification process developed from the test specimen surface inwards. In that study, the introduction of a correction was proposed, which involved substituting temperature T in Equations (4) and (5) by:

$$T = 300 + a \cdot t + \Delta T \qquad (°C) \tag{8}$$

where ΔT represents the mean difference between test specimen surface temperature (T_s) and the reference temperature measured by the kiln thermocouple (T_h), in the temperature interval at which crystallization arises.

In order to verify whether it might be convenient to operate in a similar manner in this study, a set of experiments were carried out, according to the procedure described in Section 2 of this paper, with a view to studying the way in which T_s and T_h varied, at the different tested heating rates. Tables V and VI list the resulting data.

Table V. *Variation of T_h, T_s, T_i at different heating rates (Series of experiments using frit test specimens)*

Heat- treatm. cycle	a (°C/min)	T_h (°C)	300	600	700	725	750	775	800	825	850
1	2.5	T_s (°C)	300	602	702	728	753	778	803	828	853
		T_i (°C)	296	594	693	718	743	768	793	817	842
2	5	T_s (°C)	304	603	703	728	754	779	804	829	854
		T_i (°C)	296	590	689	714	739	763	788	814	838
3	10	T_s (°C)	308	610	709	734	759	784	809	834	859
		T_i (°C)	294	587	685	710	734	758	783	807	833
4	50	T_s (°C)	302	622	718	742	766	790	815	840	865
		T_i (°C)	294	570	656	677	698	719	740	761	783

Table VI. *Variation of T_h, T_s, T_i at different heating rates. (Series of experiments using refractory test specimens)*

Heat- treatm. cycle	a (°C/min)	T_h(°C)	300	600	700	800	900	950	1000	1050	1100	1150
1	2.5	T_s (°C)	302	603	703	803	903	953	1003	1053	1104	1154
		T_i (°C)	295	595	695	795	896	946	996	1046	1096	1146
2	5	T_s (°C)	300	603	703	804	903	954	1003	1054	1104	1154
		T_i (°C)	292	592	692	792	892	942	993	1043	1093	1143
3	10	T_s (°C)	303	605	705	806	906	956	1007	1057	1107	1157
		T_i (°C)	292	589	689	789	890	940	990	1040	1090	1140
4	50	T_s (°C)	308	620	717	816	917	966	1018	1068	1117	1168
		T_i (°C)	292	585	678	774	875	923	973	1024	1075	1125

As can be observed, in all the experiments carried out, the test specimen surface temperature (T_s) was always slightly higher than the one measured by the thermocouple located within the kiln (T_h), which, as set out in Section 3.3.3, was assumed to coincide with test specimen temperature throughout the experiment. The difference observed between T_h and T_s may be due to either (or both) of two following reasons: a) as a result of the different position in respect of the kiln resistances of the thermocouples that measure both temperatures (Fig. 2); b) as a result of the welded junction of the thermocouple measuring T_h being very shiny, whereas the surface of the thermocouple where T_s is measured is dull, so that the coefficient of thermal absorption to the radiation emitted by the resistances will be greater at the test specimen surfaces than at the junction of the thermocouple measuring temperature inside the kiln, which explains why T_s is slightly higher than T_h.

In view of these results, it was decided to substitute (T) of the test specimen, in Equations (4) and (5), by Equation (8), which yields:

$$\frac{dn_z}{dt} = -A_1 \cdot \exp\left[-\frac{E_1}{R}\left(\frac{1}{573 + a \cdot t + \Delta T}\right)\right](n_z - n_z^e) \tag{9}$$

$$\frac{dn_{sz}}{dt} = A_2 \cdot \exp\left[-\frac{E_2}{R}\left(\frac{1}{573 + a \cdot t + \Delta T}\right)\right](1 - n_z - n_{sz}) \tag{10}$$

On simultaneously integrating the equations using the same boundary conditions employed for integrating Equations (6) and (7), using the values of $\Delta T=(T_s\text{-}T_h)_{mean}$ listed in Table VII, derived from the corresponding ones in Tables V and VI, the values of n_{sz} were obtained, which have been plotted in Fig. 8 (solid lines) versus *t*, together with the relevant experimental data points. It can be observed that the values of n_{sz} calculated using Equations (9) and (10), appear to fit the experimental data slightly better than when they were calculated using Equations (6) and (7).

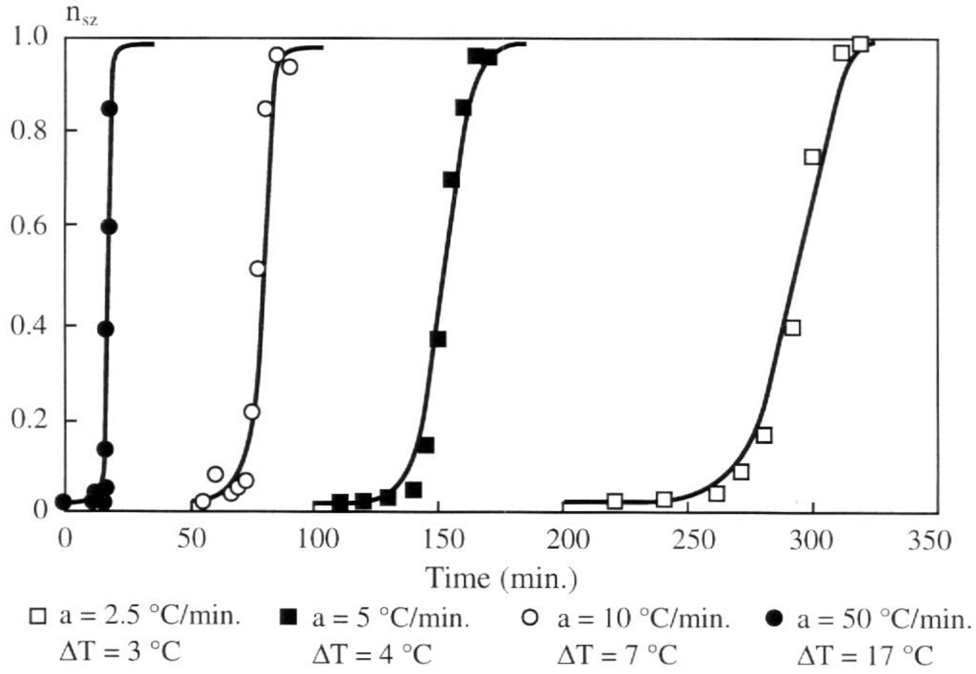

Figure 8. *Plot of the experimental data (points) and values calculated using Eqs. (9) and (10) (solid lines), for each tested heating rate.*

Table VII. *Values of ΔT used in Eqs. (6) and (7) for each studied heating rate.*

Heat-Treatment Cycle	a (°C/min)	ΔT (°C)
1	2.5	3
2	5	4
3	10	7
4	50	17

It may therefore be inferred that simultaneous integration of Equations (9) and (10) allows predicting the zirconium fraction that crystallizes as zircon, when a consolidated layer of powdered frit, of a composition and particle size like the ones studied in this paper, obtained by wet application to a ceramic body, are heated (at a constant rate of heating). This requires previously calculating the value of parameters A_1, A_2, E_1, E_2 and n^e_z (R=8,3 J/mol×K) by experiments performed under isothermal conditions, at different temperatures, with test specimens formed by casting from the selected frit and particle-size distribution. Furthermore, n^0_{oz} and n^0_{sz} must be determined, by XRD analysis, in the starting frit. The values of $\Delta T=(T_s\text{-}T_h)_{mean}$ to be used will depend on the characteristics of the kiln involved, which means that they must be measured in that kiln at the selected heating rate.

3.3.5 Justification of the temperature correction used

It follows from what has been set out that if T is replaced by T_s (test specimen surface temperature) in Equations (4) and (5), the calculated values of n_{sz} appear to match the experimental data better than if T_h is used (temperature measured by the thermocouple located inside the kiln) or T_i (temperature inside the test specimen).

This conclusion would be warranted if the crystallization phenomenon developed from the surface of the test specimen inwards, as a result of the surface receiving heat from the kiln resistances and therefore heating up from outside inwards (note that in Tables V and VI, we always find $T_i<T_s$).

In order to verify this circumstance, several experiments were carried out at the peak tested heating rate (a=50°C/min), using test specimens formed from frit particles that underwent different kiln dwell times. The evolution observed by optical microscope of the appearance of a cross-sectional area of the test specimens has been schematically illustrated in Fig. 9. It can be observed that crystal growth (diopside, zirconia, and zircon) develops from outside inwards, as expected. The fact that the growth of the crystallization region preferentially takes place from the top down, on looking at test specimens shown in Fig. 9, is due to their location in the kiln. Fig. 2 shows that the frit test specimen rests upon a refractory material base, and only receives heat by radiation from the two resistances located in the upper part of the kiln, since the other two resistances do not "see" it. Therefore, test specimen surface temperature (T_s) must be more representative of the actual temperature in the region where crystallization occurs than the temperature measured in the kiln (T_h), which is consistent with the results.

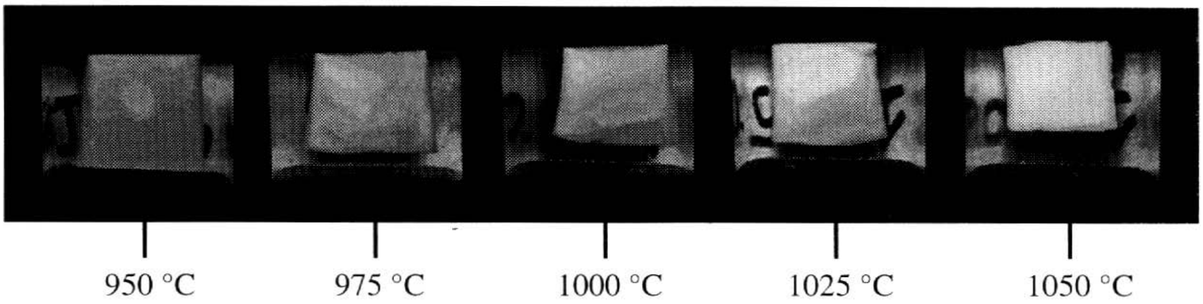

Figure 9. *Evolution of the appearance of the test specimens obtained on treating them to different peak temperatures, using a heating rate of 50°C/min.*

4. REFERENCES

[1] AMORÓS, J.L.; ESCARDINO, A.; ORTS, MªJ.; MORENO, A. Br. Ceram. Trans., 1994; 93(6); 840-844.

[2] APARICI, J.; MORENO, A.; ESCARDINO, A.; AMORÓS, J.L.; MESTRE, S.; Int.Ceram.J., December 1994; 40-44.

[3] MORENO, A.; Doctoral dissertation, Universitat Jaume I. Castellón. Spain. 1994.

[4] ESCARDINO, A.; AMORÓS, J.L.; FELÍU, C.; APARICI, C.; IV European Ceramic Conference, Rimini (Italy), 1995.